Journal of Tissues and Materials

Effect of Hydrogen Gas Pressure on the Mechanical Properties of Reduced Graphene Oxide-HA Nanocomposites

Hassan Nosrati[1], Rasoul Sarraf-Mamoory[1*], Amir Hossein Ahmadi[2], Dang Quang Svend Le[3], Maria Canillas Perez[4], Cody Eric Bünger[3]

[1]Department of Materials Engineering, Tarbiat Modares University, Tehran, Iran.
[2]Department of Basic Science, Shahed University, Tehran, Iran
[3]Department of Clinical Medicine, Aarhus University, Denmark.
[4]Instituto de Cerámica y Vidrio, CSIC, Madrid, Spain.

* Correspondence to: Sarraf-Mamoory R. (Email: rsarrafm@modares.ac.ir)

Abstract

Introduction: One of the attractive ways to synthesize graphene-hydroxyapatite (HA) nanocomposites is the hydrothermal process that results in situ synthesis of graphene-HA hybrid powders.
Objective: In this study, hydrogen gas was injected into a hydrothermal autoclave with varying initial pressures in order to investigate the effect of gas pressure on the final mechanical properties of graphene-HA nanocomposites.
Material and Methods: The powders obtained from the hydrothermal process were consolidated by spark plasma sintering method. The synthesized powders were evaluated by X-ray diffraction, Raman spectroscopy, and Fourier transform infrared spectroscopy. The sintered samples were subjected to mechanical analysis by the Vickers indentation technique.
Result: The findings of this study showed that increasing the pressure of hydrogen gas increased crystallinity, crystallite size and particle size in HA phase. Also, it increased the rate of graphene oxide reduction, increased the hardness and elastic modulus of the nanocomposites.
Conclusion: The results of this study could be useful for the synthesis and applications of graphene-HA nanocomposites.

Keyword: HA; Graphene; Indentation; Nanocomposite; Vickers

Received: 9 February 2020, **Accepted**:7 March 2020

DOI: 10.22034/jtm.2020.219321.1025

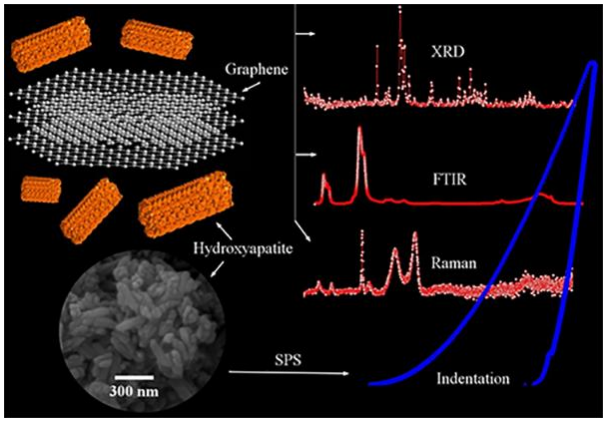

Tissues & Biomaterials Research Group

1. Introduction

Ceramics and their composites are widely used in many industries. These materials are synthesized in a variety of ways, including chemical precipitation, sol-gel, and hydrothermal process [1-3]. In the hydrothermal method, ceramics are synthesized at high temperatures and pressures and no calcination is required. One of the important applications of ceramics is medical application. Among the ceramics, the calcium phosphate family has received much attention. These materials have unique biomaterial properties such as biocompatibility and osteoconductive properties. HA is a member of this group that is very similar to the chemical structure of bone [4-13]. This ceramic is synthesized in different ways, such as combustion preparation, solid-state reaction, electrochemical deposition, sol-gel, hydrolysis, precipitation, sputtering, multiple emulsion, biomimetic deposition, solvothermal method, and hydrothermal process, and has different morphologies including rods, wires, ribbons, and tubes. It therefore has good potential for bone replacement as an implant. But despite its excellent biological properties, it is inherently brittle, has low wear resistance and, most importantly, low fracture toughness [14-32]. One of the strategies researchers have used to overcome this mechanical weakness is the use of reinforcing materials. The most popular reinforcing materials are carbon nanomaterials (carbon nanotube and graphene). And recently, graphene has outperformed.

Graphene has a honeycomb structure, has excellent mechanical properties and high specific surface area which enhances its reinforcing properties. It is biocompatible and has been widely used in research with HA. One of the attractive ways to synthesize graphene-HA nanocomposites is the hydrothermal process that results in situ synthesis of graphene-HA hybrid powders. Graphene oxide (GO) is the precursor used in this method for graphene. Anchors at the graphene oxide surface cause Van der Waals bonds with synthesized HA particles and these oxidizing agents are partially reduced by the hydrothermal process. Recently, injections of hydrogen and nitrogen gases into the autoclave have been used to increase the degree of GO reduction. The results showed that increasing the hydrothermal pressure increased the graphene oxide reduction rate and improved the HA properties [33-40].

In this study, hydrogen gas was injected into a hydrothermal autoclave with varying initial pressures. The powders obtained from this process were consolidated by spark plasma sintering method. Before examining the mechanical properties of the sintered samples, the synthesized powders were first evaluated by X-ray diffraction (XRD), Raman spectroscopy, Fourier transform infrared spectroscopy (FTIR), field emission scanning electron microscopy (FESEM), transmission electron microscopy (TEM), energy-dispersive X-ray spectroscopy (EDS), and elemental mapping methods. The sintered samples were subjected to mechanical analysis by Vickers indentation technique. For this purpose, a load of 1 N was used. It is expected that the increased pressure applied in this study will increase the mechanical properties of the nanocomposites.

Table 1. Specifications of the devices and the methods used for characterization

Method	Device and specification
XRD	X' Pert Pro, Panalytical Co., Co Kα radiation (λ=1.78901 Å)
Raman spectroscopy	Renishaw inVia spectrometer, Wavelength of 532 nm, green laser (recording 5 times for 10 seconds of each accumulation)
FTIR	VERTEX 70, Bruker Corp., applying 200 MPa pressures (1mm thickness)
FESEM	Hitachi S4700 equipped with energy dispersive X-ray spectroscopy, Au coated by sputtering
TEM	CM120, Philips

2. Experimental

The materials used in this study and the method of powder synthesis have been reported previously [34]. The hydrothermal time for the synthesis of these powders was three hours. Three samples were synthesized where the applied gas pressure for each sample was 10 (I), 20 (II), and 30 (III) bar. The synthesized powders were consolidated according to the previously reported SPS methods [34]. The amount of graphene in these nanocomposites was considered to be 1.5% by weight.

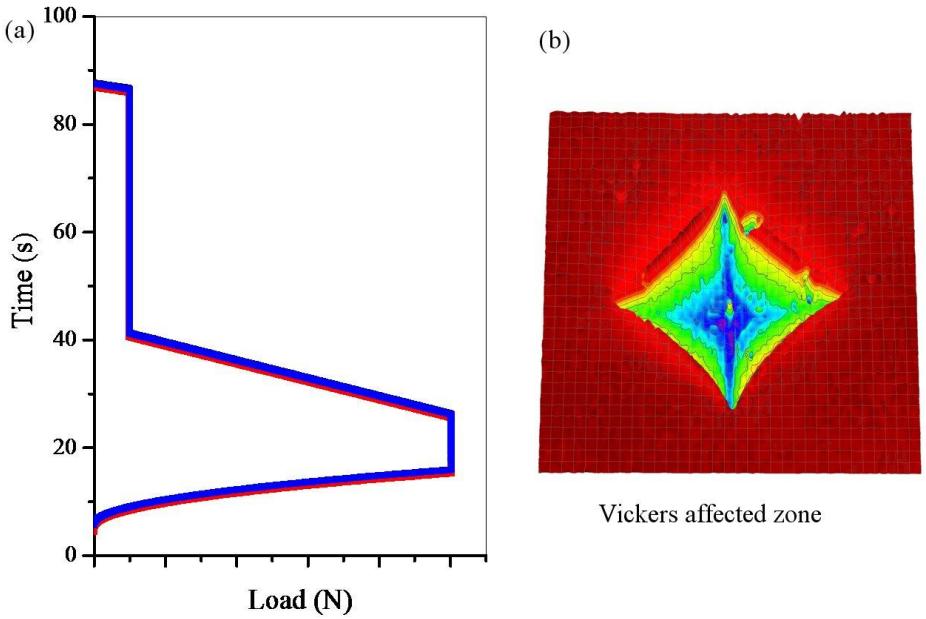

Figure 1. (a) Time-load diagram, (b) Vickers indenter affected zone

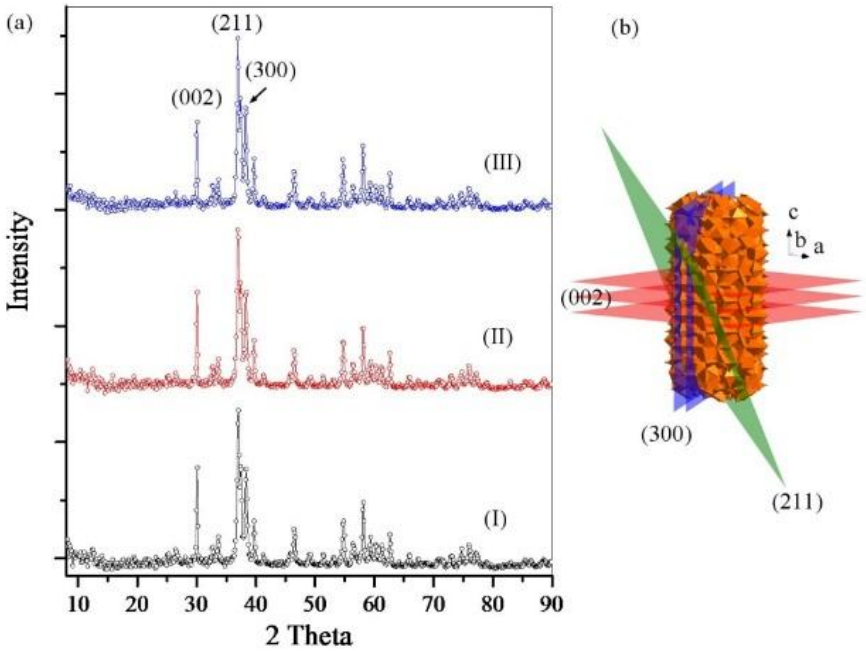

Figure 2. (a) XRD patterns of synthesized powders, (b) HA crystal structure

2.1. Characterization

The sintered samples were subjected to mechanical evaluation by Vickers indentation technique. The applied load was 10 N and the rest of the details were as reported previously [41]. Figure 1 shows the loading diagram of the mechanical evaluation along with the Vickers indenter affected zone.

Table 1 shows the specifications of the devices used for characterization. Origin pro 2016, Diamond 3.2, and ImageJ softwares were used in this study.

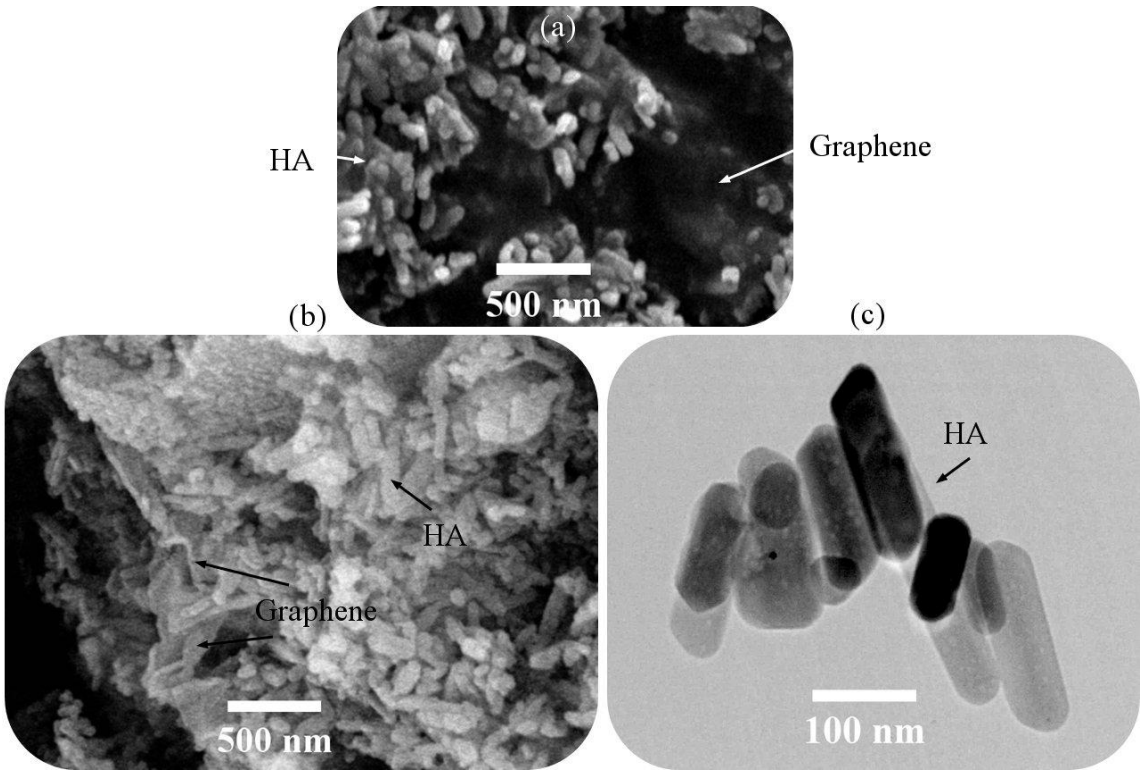

Figure 3: (a, b) FESEM images of synthesized powders (III), (c) TEM image of HA nanorods (III)

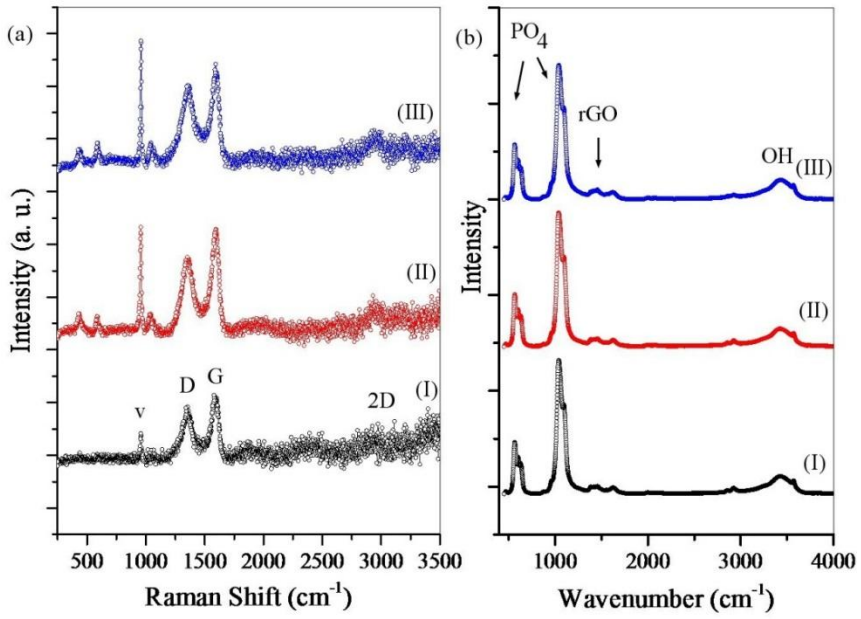

Figure 4: (a) Raman spectroscopy, (b) FTIR analysis for the synthesized powders

3. Results and discussion

Figure 2 shows the XRD patterns of synthesized powders along with the schematic image of HA crystal. As with previous published research, the patterns of all the synthesized powders are consistent with the pure HA pattern. Given the presence of GO in the precursors, and the absence of its corresponding peak at 2theta≈ 10, it can be concluded that GO has been reduced in the hydrothermal process. On the other hand, the characteristic reduced graphene oxide peak is covered with the HA (002) peak. In HA crystals, (002), (211), and (300) planes play the most role in the growth of crystals. But under the hydrothermal conditions of this research (002) planes are growing faster and causing the particle morphology to become nanorods. Increasing hydrogen gas pressure has increased the peaks intensity. This increase in pressure also affects particle size, crystallinity, and crystallite size [37, 41, 42].

Figure 3 shows the FESEM images of III powders along with the TEM image of HA nanorods in III powders. These images confirm the presence of graphene sheets in the powders. In these powders, the HA particles with nanorod morphology of about 50 nm in diameter and variable length cover the surface of the graphene sheets. Previous researches have shown that nanorods have grown in the C direction [36, 37].

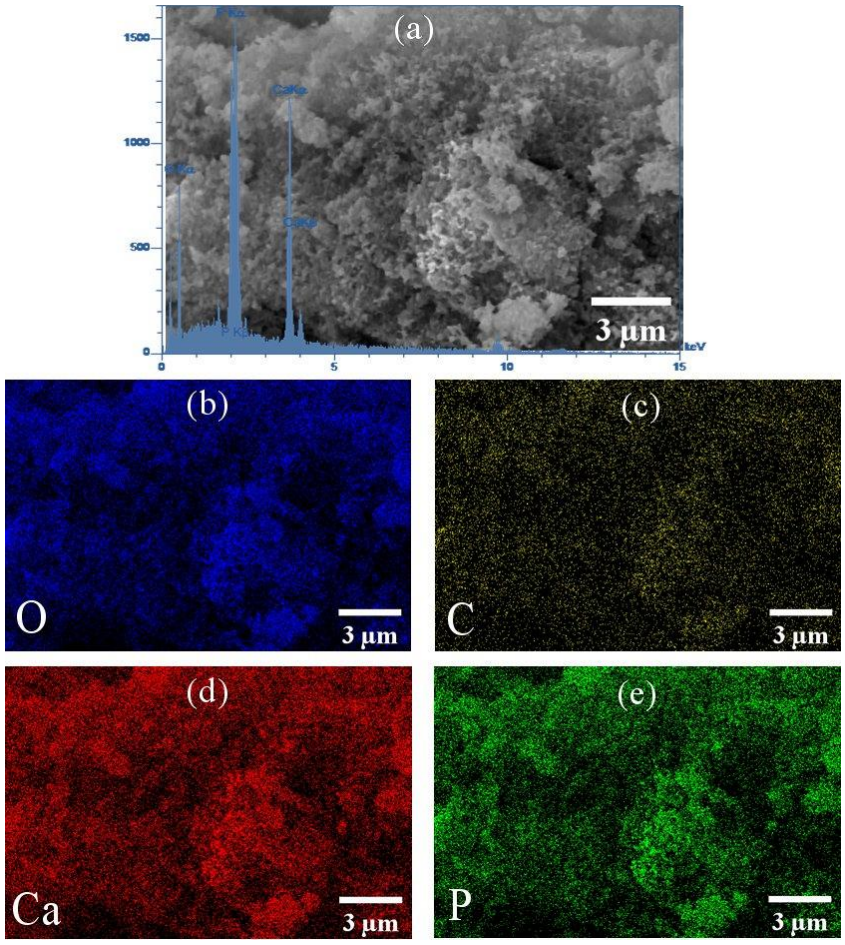

Figure 5: (a) EDS analysis (III), (b-e) elemental maps (III)

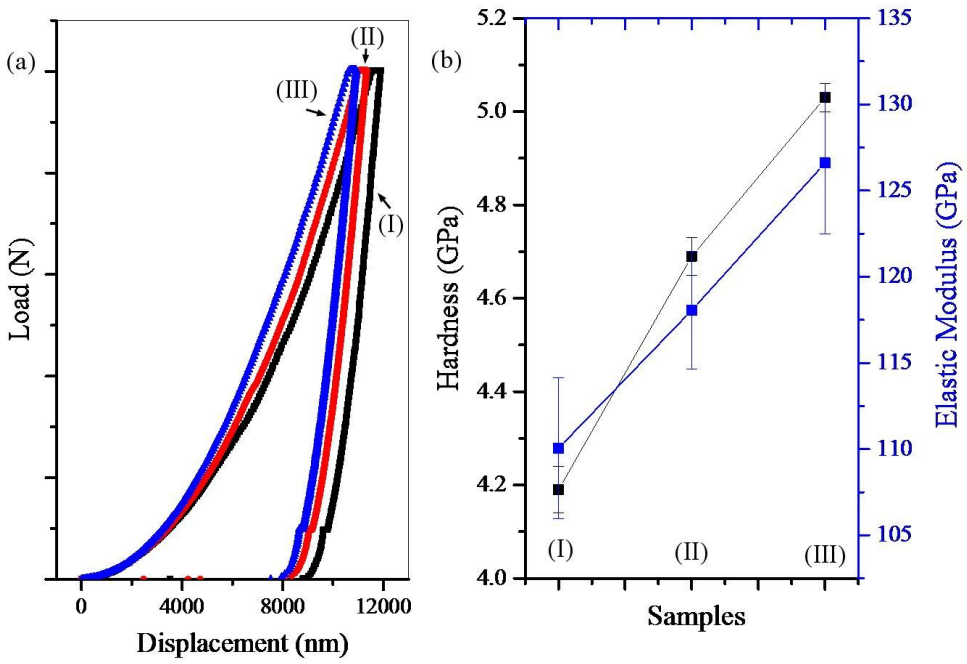

Figure 6: (a) Load-displacement diagram, (b) mechanical properties of the sintered samples

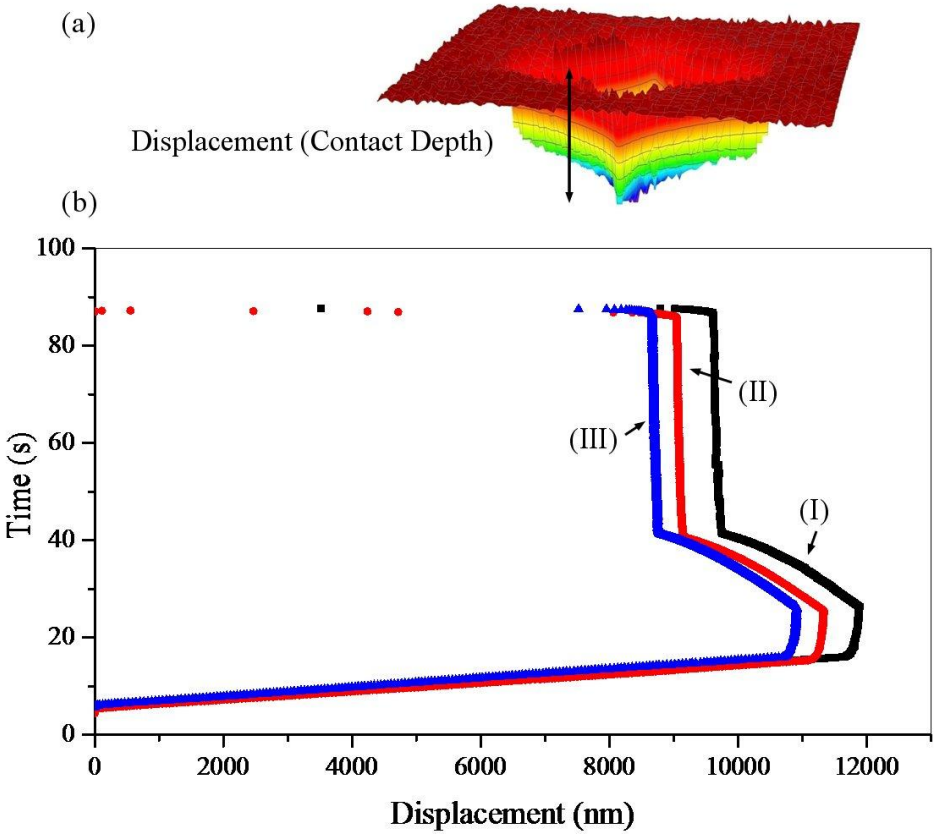

Figure 7: (a) schematic image of contact depth, (b) time-displacement diagram of the sintered samples

Figure 4 shows Raman spectroscopy and the FTIR analysis for the synthesized powders. Considering the Raman spectroscopy results (Figure 4a), it is clear that all three samples contain graphene sheets and HA. The increase in gas pressure increased the peak intensity of HA (960 cm^{-1}) due to the increase in crystallinity. Also the ID/IG ratio has increased with increasing pressure, which indicates a greater degree of reduction in GO. Considering the results of FTIR analysis (Figure 4b), all three samples are similar and only the intensity of the peaks has changed slightly. As can be seen, the characteristic peaks of graphene oxide in all three samples decreased or disappeared. These findings show that in all three samples there are two phases of reduced graphene oxide and HA. With increasing pressure, the degree of reduction is increased [41, 42].

Figure 5 shows the EDS analysis and elemental maps for III powders. This analysis confirms the presence of trace elements and the homogeneity of their distribution. Previous studies have also shown that the ratio of calcium to phosphate in these types of powders is 1.67 [37].

Figure 6 shows the load-displacement diagrams and mechanical properties of the sintered samples. As the gas pressure increases, these diagrams shift to the left and the contact depth decreases. Reducing the contact depth reduces the contact area and increases the hardness according to Olive-Pharr method [43]. Also, moving the graphs to the left increases the slope of the elastic zone and increases the elastic modulus. The results for the hardness and elastic modulus are shown in Figure 6b.

Figure 7 shows a schematic image of contact depth and the time-displacement diagram of the sintered samples. As described in the previous graphs, increasing gas pressure has increased mechanical properties and decreased contact depth. The findings of this research should be considered from two perspectives. First, the increase in gas pressure increases the HA crystallinity and increases the mechanical properties of this phase. Second, increasing gas pressure reduces the GO further and increases the mechanical properties of the recovered sheets. The findings of this study, along with other published researches, will be useful in the development of tissue engineering [44-50].

4. Conclusions

The findings of this study showed that increasing the pressure of hydrogen gas increased crystallinity, crystallite size and particle size in HA phase. Also, increasing the pressure of hydrogen gas increased the rate of GO reduction. Increasing the gas pressure in the powder synthesis section reduced the contact depth in Vickers analysis, increased the hardness and elastic modulus of the nanocomposites. The results of this study could be useful for the synthesis and applications of graphene-HA nanocomposites.

Conflict of Interests

The authors certify that they have no affiliations with or involvement in any organization or entity with any financial interest, or non-financial interest in the subject matter or materials discussed in this manuscript.

Acknowledgements

No Applicable.

References

[1] H. Nosrati, N. Ehsani, H. Baharvandi, M. Mohtashami, H. Abdizadeh, V. Mazinani, Effect of primary materials ratio and their stirring time on SiC nanoparticle production efficiency through sol-gel process, American Journal of Engineering Research (AJER) 3 (3) (2014) 317-321

[2] H. Nosrati, M. S. Hosseini, M. Nemati, A. Samariha, Production of TiO2 Nano-Rods Using Combination of Sol-Gel and Electrophoretic Methods, Asian Journal of Chemistry 25 (6) (2013) 3484-3486, http://dx.doi.org/10.14233/ajchem.2013.14250

[3] H. Nosrati, N. Ehsani, H.R. Baharvandi, H. Abdizadeh, Effect of pH on Characteristics of SiC Nanoparticles and Production Efficiency Using Chemical Method, American-Eurasian J. Agric. & Environ. Sci., 12 (5) (2012) 674-677

[4] E. Gholibegloo, A. Karbasi, M. Pourhajibagher, N. Chiniforush, A. Ramazani, T. Akbari, A. Bahador, M. Khoobi, Carnosine-graphene oxide conjugates decorated with hydroxyapatite as promising

nanocarrier for ICG loading with enhanced antibacterial effects in photodynamic therapy against Streptococcus mutans, Journal of Photochemistry & Photobiology, B: Biology 181 (2018) 14–22, https://doi.org/10.1016/j.jphotobiol.2018.02.004

[5] J.H. Lee, Y.C. Shin, S-M Lee, O.S. Jin, S.H. Kang, S.W. Hong, C-M Jeong, J.B. Huh, D-W Han, Enhanced Osteogenesis by Reduced Graphene Oxide/Hydroxyapatite Nanocomposites, Scientific Reports 5 (2015) 18833: 1-13, DOI: 10.1038/srep18833

[6] M. Jeon, S. Jung, S. Park, Facile covalent bio-conjugation of hydroxyapatite, New J. Chem. 42 (2018) 14870-14875, https://doi.org/ 10.1039/ C8NJ02766H

[7] R. Zhang, N. Metoki, O. Sharabani-Yosef, H. Zhu, N. Eliaz, Hydroxyapatite/Mesoporous Graphene/Single-Walled Carbon Nanotubes Freestanding Flexible Hybrid Membranes for Regenerative Medicine, Adv. Funct. Mater. 26 (2016) 7965–7974, DOI: 10.1002/adfm.201602088

[8] M. Ding, N. Sahebgharani, F. Musharavati, F. Jaber, E. Zalnezhad, G.H. Yoon, Synthesis and properties of HA/ZnO/CNT nanocomposite, Ceramics International 44 (2018) 7746–7753, https://doi.org/10.1016/j.ceramint.2018.01.203

[9] M. Moldovan, D. Prodan, C. Sarosi, R. Carpa, C. Socaci, M-C Rosu, S. Pruneanu, Synthesis, morpho-structural properties and antibacterial effect of silicate based composites containing graphene oxide/hydroxyapatite, Materials Chemistry and Physics 217 (2018) 48–53, https://doi.org/10.1016/j.matchemphys.2018.06.055

[10] M. Li, P. Xiong, F. Yan, S. Li, C. Ren, Z. Yin, A. Li, H. Li, X. Ji, Y. Zheng , Y. Cheng, An overview of graphene-based hydroxyapatite composites for orthopedic applications, Bioactive Materials 3 (2018) 1-18, https://doi.org/10.1016/j.bioactmat.2018.01.001

[11] C. Gao, P. Feng, S. Peng, C. Shuai, Carbon nanotube, graphene and boron nitride nanotube reinforced bioactive ceramics for bone repair, Acta Biomaterialia 61 (2017) 1–20, http://dx.doi.org/10.1016/j.actbio.2017.05.020

[12] J.J. Lee, Y.C. Shin, S-J Song, J.M. Cha, S.W. Hong, Y-J Lim, S.J. Jeong, D-W Han, B. Kim, Dicalcium Phosphate Coated with Graphene Synergistically Increases Osteogenic Differentiation In Vitro, Coatings 8 (13) (2018) 1-12, doi:10.3390/coatings8010013

[13] Y. Zeng, X. Pei, S. Yang, H. Qin, H. Cai, S. Hu, L. Sui, Q. Wan, J. Wang, Graphene oxide/hydroxyapatite composite coatings fabricated by electrochemical deposition, Surface & Coatings Technology 286 (2016) 72–79, http://dx.doi.org/10.1016/j.surfcoat.2015.12.013

[14] M. Canillas, R. Rivero, R. García-Carrodeguas, F. Barba, M.A. Rodríguez, Processing of hydroxyapatite obtained by combustion synthesis, Boletín de la Sociedad Española de Cerámica y Vidrio 56 (5) (2017) 237-242, https:// doi.org/ 10.1016/ j.bsecv.2017.05.002

[15] X. Guo, H. Yan, S. Zhao, L. Zhang, Y. Li, X. Liang, Effect of calcining temperature on particle size of hydroxyapatite synthesized by solid-state reaction at room temperature, Advanced Powder Technology 4 (6) (2013) 1034-1038, https://doi.org/10.1016/j.apt.2013.03.002

[16] M. Shikhanzadeh, Direct formation of nanophase hydroxyapatite on cathodically polarized electrodes., J Mater Sci: Mater Med. 9 (1998) 67-72, http://dx.doi.org/10.1023/A:1008838813120

[17] A. Jillavenkatesa, R.A. Condrate Sr., Sol–gel processing of hydroxyapatite, J. Mater. Sci. 33 (1998) 4111–4119, https://doi.org/10.1023/A:1004436732282

[18] T.A. Kuriakosea, S.N. Kalkura, M. Palanichami, D. Arivuoli, K. Dierks, G. Bocelli, C. Betzel, Synthesis of stoichiometric nano crystalline hydroxyapatite by ethanol-based sol–gel technique at low temperature, Journal of Crystal Growth 263 (1-4) (2004) pp. 517-523, https://doi.org/10.1016/j.jcrysgro.2003.11.057

[19] O. V. Sinitsyna, A. G. Veresov, E. S. Kovaleva, Y. V. Kolen'ko, V. L. Putlyaev, Y. D. Tretyakov, Synthesis of hydroxyapatite by hydrolysis of α-Ca3(PO4)2, Russian Chemical Bulletin 54 (1) (2005) 79-86, https://doi.org/10.1007/s11172-005-0220-9

[20] C. Liu, Y. Huang, W. Shen, J. Cui, Kinetics of hydroxyapatite precipitation at pH 10 to 11, Biomaterials 22 (4) (2000) 301-306, https://doi.org/10.1016/S0142-9612(00)00166-6

[21] C.M. Manuel, M.P. Ferraz, F.J. Monteiro, Synthesis of hydroxyapatite and tri calcium phosphate nanoparticles Preliminary Studies, Key Eng Mater. 240-242 (2003) 555-558, https://doi.org/10.4028/www.scientific.net/KEM.240-242.555

[22] K. Yamashita, T. Arashi, K. Kitagaki, S. Yamada, T. Umegaki, Preparation of apatite thin films through rfsputtering from calcium phosphate glasses, J. Am. Ceram. Soc. 77 (9) (1994) 2401–2407, https://doi.org/10.1111/j.1151-2916.1994.tb04611.x

[23] I. Kimura, Synthesis of hydroxyapatite by interfacial reaction in a multiple emulsion, Res Lett Mater Sci. (2007) 1-4, http://dx.doi.org/10.1155/2007/71284

[24] A.C. Tas, Synthesis of biomimetic Ca-hydroxyapatite powders at 37 degrees C in synthetic body fluids, Biomaterials 21 (2000) 1429-1438, http://dx.doi.org/10.1016/S0142-9612(00)00019-3

[25] C. Qi, Y-J Zhu, G-J Ding, J. Wu, F. Chen, Solvothermal synthesis of hydroxyapatite nanostructures with various morphologies using adenosine 50-monophosphate sodium salt as an organic phosphorus source, RSC Adv. 5 (2015) 3792-3798, DOI: 10.1039/c4ra13151g

[26] I.S. Neira, Y.V. Kolen'ko, O.I. Lebedev, G. Van Tendeloo, H.S. Gupta, F. Guitián, M. Yoshimura, An Effective Morphology Control of Hydroxyapatite Crystals via Hydrothermal Synthesis, Cryst. Growth Des. 9 (1) (2009) 466-474, https://doi.org/10.1021/cg800738a

[27] F. Peng, X. Yu, M. Wei, In vitro cell performance on hydroxyapatite particles/poly(l-lactic acid) nanofibrous scaffolds with an excellent particle along nanofiber orientation, Acta Biomater. 7 (2011) 2585–2592, https://doi.org/10.1016/j.actbio.2011.02.021

[28] M. Jevtić, M. Mitrić, S. Škapin, B. Jančar, N. Ignjatović, D. Uskoković, Crystal Structure of Hydroxyapatite Nanorods Synthesized by Sonochemical Homogeneous Precipitation, Cryst. Growth Des 8 (2008) 2217–2222, https://doi.org/10.1021/cg7007304

[29] D.O. Costa, S.J. Dixon, A.S. Rizkalla, One- and Three-Dimensional Growth of Hydroxyapatite Nanowires during Sol–Gel–Hydrothermal Synthesis, ACS Appl Mater Interfaces 4 (2012) 1490–1499, https://doi.org/10.1021/am201735k

[30] Y. Zhang, J. Lu, J. Wang, S. Yang, Y. Chen, Synthesis of nanorod and needle-like hydroxyapatite crystal and role of pH adjustment, J. Cryst. Growth 311 (2009) 4740–4746, https://doi.org/10.1016/j.jcrysgro.2009.09.018

[31] B.B. Chandanshive, P. Rai, A.L. Rossi, O. Ersen, D. Khushalani, Synthesis of hydroxyapatite nanotubes for biomedical applications, Mater Sci Eng C 33 (2013) 2981–2986, https://doi.org/10.1016/j.msec.2013.03.022

[32] Q. Sun, J. T. Lou, F. Kang, J. F. Chen, J. X. Wang, Facile preparation of hydroxyapatite nanotubes assisted by needle-like calcium carbonate, Powder Technol. 261 (2014) 49–54, https://doi.org/10.1016/j.powtec.2014.04.014

[33] H. Nosrati, R. Sarraf-Mamoory, F. Dabir, Crystallographic study of hydrothermal synthesis of hydroxyapatite nano-rods using Brushite precursors, Journal of Tissues and Materials 2 (3) (2019) 1-8, DOI: 10.22034/jtm.2019.199830.1022

[34] H. Nosrati, R. Sarraf-Mamoory, D. Q. S. Le, C. E. Bunger, Preparation of reduced graphene oxide/hydroxyapatite nanocomposite and evaluation of graphene sheets/hydroxyapatite interface, Diamond & Related Materials 100 (2019) 107561, https://doi.org/10.1016/j.diamond.2019.107561

[35] H. Nosrati, R. Sarraf Mamoory, F. Dabir, M. C. Perez, M. A. Rodriguez, D. Q. S. Le, C. E. Bünger, In situ synthesis of three dimensional graphene/hydroxyapatite nano powders via hydrothermal process, Materials Chemistry and Physics 222 (2019) 251–255, https://doi.org/10.1016/j.matchemphys.2018.10.023

[36] H. Nosrati, R. Sarraf Mamoory, F. Dabir, D. Q. S. Le, C. E. Bunger, M. C. Perez, M. A. Rodriguez, Effects of hydrothermal pressure on in situ synthesis of 3D graphene/hydroxyapatite nano structured powders, Ceramics International 45 (2019) 1761–1769, https://doi.org/10.1016/j.ceramint.2018.10.059

[37] H. Nosrati, R. Sarraf-Mamoory, D. Q. S. Le, C. E. Bunger, Fabrication of gelatin/hydroxyapatite/3D-graphene scaffolds by a hydrogel 3D-printing method, Materials Chemistry and Physics 239 (2020) 122305, https://doi.org/10.1016/j.matchemphys.2019.122305

[38] A. H. Ahmadi, H. Nosrati, R. Sarraf-Mamoory, Decreasing β- three calcium phosphate particle size using graphite as nucleation sites and diethylene glycol as a chemical additive, Journal of Bioengineering Research 1(4) (2020), DOI:10.22034/JBR.2019.211371.1016

[39] H. Nosrati, R. Sarraf-Mamoory, D.Q.S. Le, M. Canillas Perez, C. Bunger, Studying the physical behavior of human mesenchymal stem cells on the surface of hydroxyapatite after adding graphene as a reinforcement, Journal of Bioengineering Research (2020), doi: 10.22034/jbr.2019.213164.1018

[40] H. Nosrati, D. Q. S. Le, R. Z. Emameh, C. E. Bunger, Characterization of the precipitated Dicalcium Phosphate Dehydrate on the Graphene Oxide surface as a bone cement reinforcement, Journal of Tissues and Materials 2 (1) (2019) 33-46, DOI: 10.22034/jtm.2019.173565.1013

[41] H. Nosrati, R. Sarraf Mamoory, D. Q. S. Le, C. E. Bunger, R. Zolfaghari Emameh, F. Dabir, Gas injection approach for synthesis of hydroxyapatite nanorods via hydrothermal method, Materials Characterization 2019; 110071, https://doi.org/10.1016/j.matchar.2019.110071

[42] S. Baradaran, E. Moghaddam, W.J. Basirun, M. Mehrali, M. Sookhakian, M. Hamdi, et al, Mechanical properties and biomedical application of a nanotube hydroxyapatite-reduced graphene oxide composite, Carbon 69 (2014) 32–45, http://dx.doi.org/10.1016/j.carbon.2013.11.054

[43] W. Oliver, G. Pharr, An improved technique for determining hardness and elastic modulus using load and displacement sensing indentation experiments, J. Mater. Res. 7 (1992) 1564–1583.

[44] H. Nosrati, R. Sarraf-Mamoory, D.Q.S. Le, C.E. Bünger, Enhanced fracture toughness of three dimensional graphene- hydroxyapatite nanocomposites by employing the Taguchi method, Composites Part B: Engineering 190 (2020) 107928; https://doi.org/10.1016/j.compositesb.2020.107928

[45] H. Nosrati, R. Sarraf-Mamoory, D.Q.S. Le, M.C. Perez, C.E. Bünger, Evaluation of Argon-Gas-Injected Solvothermal Synthesis of Hydroxyapatite Crystals Followed by High-Frequency Induction Heat Sintering, Cryst. Growth Des. 20(5) (2020) 3182-3189; https://doi.org/10.1021/acs.cgd.0c00048

[46] H. Nosrati, R. Sarraf-Mamoory, A.H. Ahmadi, M.C. Perez, Synthesis of Graphene Nanoribbons–Hydroxyapatite Nanocomposite Applicable in Biomedicine and Theranostics, J. Nanotheranostics 1(1) (2020) 2; https://doi.org/10.3390/jnt1010002

[47] A. Aidun, A.S. Firoozabady, M. Moharrami, A. Ahmadi, N. Haghighipour, S. Bonakdar, Graphene oxide incorporated polycaprolactone/chitosan/collagen electrospun scaffold: Enhanced osteogenic properties for bone tissue engineering, Artifical Organs 43(10) (2019) 264-281; https://doi.org/10.1111/aor.13474

[48] F. Ghorbani, A. Zamanian, A. Shams, A. Shamoosi, A. Aidun, Fabrication and characterisation of super-paramagnetic responsive PLGA–gelatine–magnetite scaffolds with the unidirectional porous structure: a physicochemical, mechanical, and in vitro evaluation, IET Nanobiotechnology 13(8) (2019) 860 – 867; https://doi.org/10.1049/iet-nbt.2018.5305

[49] H.Z. Marzouni, F. Tarkhan, A. Aidun, K. Shahzamani, H.R. Jahan Tigh, S. Malekshahian, H.E. Lashgarian, Cytotoxic Effects of Coated Gold Nanoparticles on PC12 Cancer Cell, Galen Medical Journal 7 (2018); http://dx.doi.org/10.22086/gmj.v0i0.1110

[50] A. Aidun, A. Zamanian, F. Ghorbani, Immobilization of polyvinyl alcohol-siloxane on the oxygen plasma-modified polyurethane-carbon nanotube composite matrix, Applied Polymer 137(12) (2020) 48477; https://doi.org/10.1002/app.48477